Direct photons in the UA2 Detector

The UA2 Collaboration
Bern - Cambridge - CERN - Dortmund - Heidelberg - Melbourne
Milano - Orsay (LAL) - Pavia - Perugia - Pisa - Saclay (CEN)

Presented by
Cinzia Talamonti
University of Perugia and INFN Sezione di Perugia - Italy

Abstract

New results on single and double prompt photon production in $\overline{p}p$ interactions are presented. The data sample corresponds to an integrated luminosity of 13.2 pb^{-1} accumulated during the 1988-1990 UA2 runs. The results are in good agreement with the predictions of perturbative QCD.

1 Introduction

The study of high transverse momentum (p_T) photon production is a convenient way to extract information about the constituents of hadronic matter and their interactions. A measurement of the direct photon cross-section is a good test of QCD with the advantage that the photon p_T is not affected by fragmentation effects, resulting in experimental uncertainties which are smaller than those obtained in the measurement of a jet cross-section. Next-to-leading order calculations for both single and double prompt photon production are available [2]-[3]to be compared to the experimental results.

The direct production of high p_T photons from hadron-hadron collisions is described in the Born approximation by $q\overline{q}$ annihilation and the Compton process $gq \rightarrow \gamma q(or\ g\overline{q} \rightarrow \gamma\overline{q})$. A further contribution from quark bremsstrahlung is experimentally suppressed by the requirement of a well isolated photon in the final state. The main contributions to double direct photon production come from $q\overline{q}$ annihilation, $gg \rightarrow \gamma\gamma$ interaction and from bremsstrahlung.

The main source of background to the photon signal comes from π^0 or η decays into photon pairs that cannot be resolved at high energy. This background is overwhelming because of the low production cross-section of direct photon processes with respect to jet production. An isolation requirement is very powerful in reducing this background, since π^0 and η from jets are accompaned by jet fragments, while prompt photon production results in isolated electromagnetic clusters.

This report is organized as follows: Section 2 describes the photon identification criteria and the method used for background subtraction, while the calculation of single and double prompt photon cross-section is presented in section 3 and 4, respectively.

2 Photon selection and background subtraction

The UA2 detector has been extensively described in Ref.[1]. This analysis [4] has been performed only in the central region of the detector. A photon candidate is identified as an electromagnetic cluster well contained in the electromagnetic calorimeter satisfying the following criteria :

- Lateral and longitudinal profiles of the cluster consistent with that expected from a single isolated electron or photon.
- The absence of charged tracks in front of the calorimeter cluster in a window of $\Delta\eta < 0.2$ and $\Delta\phi < 15°$ about the cluster axis (defined by the line joining the interaction vertex to the cluster centroid).
- At most one preshower signal in a cone $\sqrt{\Delta\phi^2 + \Delta\eta^2} < 0.265$ about the cluster axis.

According to the presence or absence of a signal in the preshower detector the photon is defined as converted or unconverted. The isolation criteria reduce the contamination from hadronic jets and photons coming from quark bremsstrahlung, while keeping a high efficiency for direct photons. The residual background contamination is measured and subtracted on a statistical basis, by considering the fraction α of photons in the sample that initiate showers in the converter of the preshower detector. The conversion probability α in the sample is then computed as :

$$\alpha = \frac{N_c^{true}}{N_c^{true} + N_u^{true}}$$

where (N_c^{true}) and (N_u^{true}) are the true numbers of converted and unconverted photons determined from the number of observed photon candidates after corrections for all the selection efficiencies which have a different value for converted and unconverted photons [4].

The conversion probability ε_γ of an incident single photon is evaluated as a function of the photon energy. using the EGS shower simulation programe [5]. The multiphoton conversion probability ε_π for photon pairs produced by single π^0 and η decays is calculated by Monte Carlo using ε_γ for each photon and assuming that the ratio between the number of π^0 and η is 0.6 and p_T independent [6]. The calculated values of ε_π and ε_γ are compared in Fig. 2a with the measured conversion probability α as a function of the cluster energy E_γ : the measured values lie between the two theoretical curves and tend towards ε_γ as E_γ increases.

The fraction of multiphoton events in the sample,

$$b(p_T) = \frac{\alpha - \varepsilon_\gamma}{\varepsilon_\pi - \varepsilon_\gamma}$$

computed in each p_T–bin is shown in Fig. 2b to decrease with increasing p_T.

3 Single photon inclusive cross–section

To estimate the single photon inclusive cross-section only events with a single reconstructed $\overline{p}p$ interaction vertex and having an electromagnetic cluster well contained in a fiducial region of the central calorimeter ($|\ \eta\ | < 0.76$) are considered. In addition, such a cluster must have the characteristics expected for an isolated single photon and a $p_T > 15$ GeV.

The invariant inclusive cross–section for direct photon production is evaluated from

$$E\frac{d\sigma}{d^3p} = \frac{N_\gamma(p_T) \cdot [1 - b(p_T)]}{2\pi\ p_T\ \Delta p_T\ \mathcal{L}\ \varepsilon_c\ A(p_T)}$$

where $N_\gamma(p_T)$ is the number of photon candidates in a p_T–bin of width Δp_T, $b(p_T)$ is the background fraction in that bin, $\mathcal{L} = 13.2 \pm 0.7\ pb^{-1}$ is the integrated luminosity corresponding to the data sample, $\epsilon_c = 0.454 \pm 0.011$ is the direct photon detection efficiency and $A(p_T)$ is the geometrical acceptance. A background from beam halo particles has been estimated to be less than 1% of the photon candidate sample at all p_T and has been neglected. The contribution from $W \to e\nu$ decays where no electron track was reconstructed is estimated to be [4] 0.2% of the photon candidates in the p_T region between 20 and 45 GeV and is also neglected.

The results are compared to next–to–leading order QCD calculations [2] performed using different sets of structure functions [7]. The isolation cut suppresses the bremsstrahlung contribution from final state quarks and is therefore included in the QCD calculation (see Ref. [2] for a description of the exact procedure). The p_T distribution of the data together with the QCD expectations is shown in Fig. 2. The error bars indicate the statistical and p_T dependent systematic uncertainties added in quadrature. Not included in Fig. 2 is an overall p_T independent systematic error of 9%. Within these uncertainties, the data agree with the QCD predictions, but a more accurate theoretical estimate of the bremsstrahlung contribution is needed for a better quantitative comparison.

4 Double photon inclusive cross–section

The double prompt photon inclusive cross-section has been estimated selecting events having two electromagnetic clusters (γ_1 and γ_2) in the central calorimeter with an azimuthal separation of at least 60^0.The electromagnetic clusters must satisfy the following requirements:

- $P_T(\gamma_1) > 10\ GeV$ and $P_T(\gamma_2) > 9\ GeV$;
- $|\eta(\gamma_1)| < 0.76$ and $|\eta(\gamma_2)| < 0.76$;
- Z > 0.7 where Z is defined as

$$Z = -\frac{\vec{p}_T(\gamma_1) \cdot \vec{p}_T(\gamma_2)}{|p_T(\gamma_1)|^2}$$

This last cut rejects the events with a large imbalance between the P_T of the two clusters. In this way the contribution from quark bremsstrahlung processes is reduced, as well as the background from jet events in which part of the jet energy falls outside the reconstructed cluster.

Photon identification cuts are then applied to each of the two electromagnetic clusters in order to select the final two–photon candidate sample. These criteria and the background subtraction are based on the same principles as the ones applied in the single photon analysis.

The invariant inclusive cross-section for double prompt photon production is evaluated from

$$\frac{d\sigma_{\gamma\gamma}}{dp_T} = \frac{N^*_{\gamma\gamma}}{\varepsilon_C^2\ A(p_T)\ \Delta p_T\ \mathcal{L}}$$

where $N^*_{\gamma\gamma}$ is the number of photons in each bin, ε_C is the efficiency of the cuts defining an electromagnetic cluster, $A(p_T)$ is the geometrical acceptance, Δp_T is the bin size and $\mathcal{L}$ is the integrated luminosity. Values of the cross-section for double prompt photon production, $d\sigma_{\gamma\gamma}/dp_T$ are obtained from the number of photons falling inside a given p_T bin when the event contains a second photon. With this definition, each event is counted twice, once for each p_T bin to which the two photons belong. The cross-section values so obtained are shown in Fig. 4. The quoted errors include the statistical and all p_T-dependent systematic uncertainties. In addition, there is a normalization uncertainty of 6.8%. Fig. 4 shows also the results of two independent QCD predictions to next-to-leading order (NLO). The calculation of Ref. [8] is performed analytically, whereas a MonteCarlo method is used for Ref. [3]. In the two cases the same parameters are used: a NLO definition of α_s; the HMRSB structure functions [9] ; $Q^2 = p_T^2$; and no isolation criteria on the photon. However, while the calculation of Ref. [3] is performed by requiring $|\ \eta\ | < 0.76$ for both photons, as in the data, in the analytical calculation of Ref. [8] this requirement is applied to only one photon, resulting in a cross-section which is larger by approximately a factor of 2.5. The result of this calculation was therefore corrected for the reduced acceptance of the data using the MonteCarlo simulation described above. For both predictions the agreement is good apart from the first bin in p_T where the data lie significantly above the theoretical prediction. This discrepancy could be due to the theoretical uncertainties in the calculation of the diagrams where the final state photons are radiated from quarks (bremsstrahlung diagrams), which contribute mostly in the lowest p_T bin.

References

[1] UA2 Collaboration, C. N. Booth, Proc. 6th Topical Workshop on $\bar{p}p$ Collider Physics (Aachen, 1986), eds. K. Eggert et al. (World Scientific, Singapore, 1987) p. 381.

[2] P.Aurenche et al.: Phys. Lett.**B140** (1984) 87; P.Aurenche et al.: Nucl. Phys.**B297** (1988) 661; P.Aurenche et al.: Phys. Rev.**D42** (1990) 1440.

[3] B.Bailey,J. Ohnemus,and J.F. Owens, FSUHEP-920320 and DTP/92/18.

[4] UA2 Collaboration, J. Alitti et al., Phys.Lett. **B263** (1991) 544.

[5] R. Ford and W. Nelson, SLAC-210 (1978).

[6] UA2 Collaboration, M. Banner et al., Z. Phys. **C27** (1985) 329.

[7] D.W. Duke and Owens, Phys. Rev. **D30** (1984) 49; E. Eichten et al.: Rev. Mod. Phys. **56** (1984) 579; erratum Rev. Mod. Phys. **58** (1986) 1065; P. Aurenche et al.: Phys. Rev. **D39** (1989) 3275.

[8] P. Aurenche et al.: Z. Phys. **C29** (1985) 459.

[9] P.N. Harriman, A.D. Martin, R.G. Roberts, and W.J. Stirling, Phys. Rev. **D42** (1990); Phys. Lett. **B243** (1990) 421.

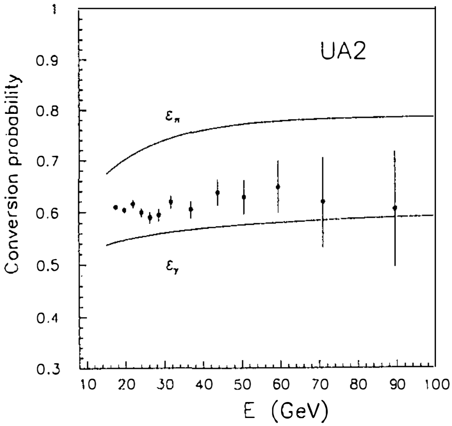

Figure 1
Conversion fraction for photon candidates

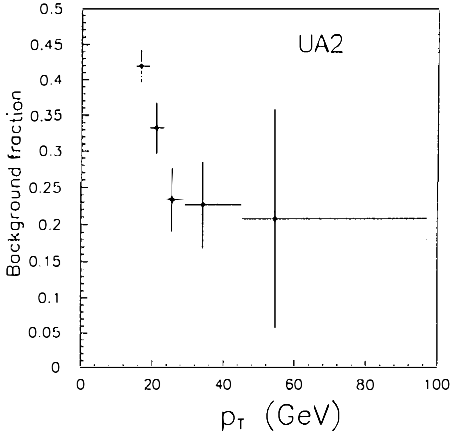

Figure 2
The fractional multiphoton background contamination in the sample of candidates events

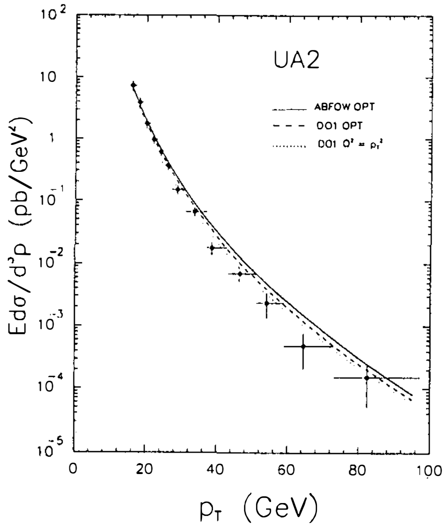

Figure 3
The invariant cross section for direct photon production compared with QCD calculations

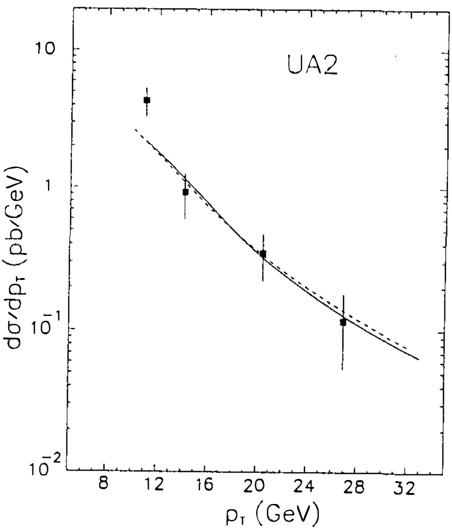

Figure 4
Differential double promp photon cross-section compared with QCD predictions